Published in final edited form as:
Langmuir. 2002 January 8; 18(1): 231–238. doi:10.1021/la010937t.

N-Myristoylated Phosphatidylethanolamine: Interfacial Behavior and Interaction with Cholesterol

Xin-Min Li[†], **M. Ramakrishnan**[‡], **Howard L. Brockman**[†], **Rhoderick E. Brown**[*,†], and **Musti J. Swamy**[*,‡]
The Hormel Institute, University of Minnesota, Austin, Minnesota 55912, and School of Chemistry, University of Hyderabad, Hyderabad - 500 046, India

Abstract

The interfacial packing behavior of *N*-myristoyldimyristoylphosphatidylethanolamine (*N*-14:0 DMPE) and its interaction with cholesterol were characterized and compared to the behavior of dimyristoylphosphatidylethanolamine (DMPE) using an automated Langmuir type film balance. Surface pressure and surface potential were monitored as a function of lipid cross-sectional molecular area. *N*-14:0 DMPE exhibited two-dimensional (2D) phase transitions of a liquid-expanded to condensed nature at many temperatures in the 15-30 °C range, but isotherms showed only condensed behavior at 15 °C. The sharp decline in the surface compressional moduli upon entering the 2D-transition region is consistent with differences in the partial molar areas of coexisting liquid-expanded (chain-disordered) and condensed (chain-ordered) phases. Including Ca^{2+} in the subphase beneath the negatively charged *N*-14:0 DMPE caused a downward shift in the 2D-transition onset pressure even in the presence of 100 mM NaCl. The average dipole moments perpendicular to the lipid-water interface for *N*-14:0 DMPE's liquid-expanded and condensed phases were higher than those of DMPE. At surface pressures sufficiently low (<10 mN/m) to produce liquid-expanded phase behavior in pure *N*-14:0 DMPE, mixing with cholesterol resulted in a classic “condensing effect”. Maximal area condensation was observed near equimolar *N*-14:0 DMPE/cholesterol. Insights into mixing behavior at high surface pressures that mimic the lipid cross-sectional areas of biomembranes were provided by analyzing the surface compressional moduli as a function of cholesterol mole fraction. Complex mixing patterns were observed that deviated significantly from theoretical ideal mixing behavior suggesting the presence of lipid “complexes” and/or a liquid-ordered phase at high sterol mole fractions (>0.35) and low to intermediate surface pressures (<20 mN/m) as well as the possible coexistence of relatively immiscible solid phases at higher surface pressures (e.g., 35 mN/m).

Introduction

N-Acylphosphatidylethanolamines (NAPEs) are naturally occurring derivatives of phosphatidylethanolamine (PE), in which the amino group is derivatized with a long acyl chain.[1] NAPEs are present in a variety of species including microbes, plants, and animals.[2-12] While PE is a major plasma membrane lipid in many organisms, NAPEs are normally present in only very small quantities. The content of NAPEs and *N*-acylethanolamines (NAEs) increases dramatically when the tissue is subjected to a condition of stress, such as wounding in animals or dehydration in plant tissues.[1] This increase could be part of a stress-fighting response of the

[*]Corresponding authors. Dr. Rhoderick E. Brown: e-mail, reb@tc.umn.edu; fax, +1-507-437-9606; tel, +1-507-433-8804. Dr. Musti J. Swamy: e-mail, mjssc@uohyd.ernet.in; fax, +91-40-301-2460/ 0145/ 0120; tel, +91-40-301-0500 ext 4807..
[†]University of Minnesota.
[‡]University of Hyderabad.

parent organism. NAPEs are precursors to NAEs which may act as neurotransmitters or second messengers.[1,13] Consistent with this hypothesis, NAEs accumulate in infarcted canine myocardium and ischemic rat brain.[10,12] In cultured cells, serum deprivation leads to an increase in the content of both NAPEs and NAEs, which return to normal levels upon restoration of serum in the culture medium.[14] In cultured neurons, the neurotoxic amino acid glutamate induces formation of NAPE and NAE in a dose-dependent manner,[15,16] while treatment of cultured tobacco cells with xylanase, a fungal elicitor, results in NAE accumulation in the culture medium.[17] These observations suggest that stress-induced accumulation of NAPEs and NAEs may be a stress-fighting or defense response of the parent organisms/cells. In addition, NAPEs are potentially useful in developing liposomal drug delivery systems since they stabilize liposomes even in the presence of human serum.[18,19]

In view of the foregoing, it is important to investigate the properties of NAPEs and their interaction with other membrane lipids. Freeze-fracture electron microscopy (EM) has shown that *N*-lauroyl DLPE forms liposomes in aqueous media, while ^{31}P NMR and freeze-fracture EM studies have shown that *N*-acyl DPPEs with acyl chain lengths from 2 to 18 C atoms form lamellar structures in the gel and fluid phases.[20-23] Differential scanning calorimetry (DSC), Fourier transform infrared reflectance (FTIR), and ^{31}P NMR studies on *N*-acyl DPPEs have revealed that the *N*-acyl chain of these lipids folds back and integrates into the membrane interior when its length is ≥ 10 C atoms, whereas shorter chains are in contact with the aqueous environment at the membrane interface.[21,22,24] Also, it has been shown by attenuated total reflectance FTIR spectroscopy that the *N*-acyl chain of *N*-16:0 DPPE is oriented parallel to the *O*-acyl chains, whereas the *N*-acyl chain of *N*-6:0 DPPE is randomly oriented.[25] DSC studies on NAPEs with matched *N*- and *O*-acyl chains have shown that the contribution of the *N*-acyl chain to the chain-melting enthalpy of the lipid is considerably smaller than that of the *O*-acyl chains, suggesting that the packing of the *N*-acyl chains differs from that of the *O*-acyl chains.[23,26] Spin-label electron spin resonance (ESR) studies have shown that the *N*-acyl chain of NAPEs with matched *N*- and *O*-acyl chains lies at nearly the same vertical location as that of the *sn*-2 (*O*) acyl chain and that the condensing effect of cholesterol is felt equally by the *N*-acyl and *sn*-2 (*O*) acyl chains.[27] Very recently, the mixing behavior of *N*-14:0 DMPE with DMPC has been investigated by DSC.[28]

Since embedding of the long *N*-acyl chain into the membrane may be involved in the stress-fighting mechanism, possibly by altering the membrane properties in stress-countering ways, it is important to study the properties of membranes made up of pure NAPEs as well as those that contain mixtures of NAPEs and other major membrane lipids such as PC, PE, and cholesterol. Such studies are important because of the ubiquitous presence of this sterol in the plasma membrane of different species and in view of the changes in NAPE content in different organisms subjected to stress. Here, we have investigated the monolayer properties of *N*-14:0 DMPE and its interaction with cholesterol and compared the response to that of DMPE using the Langmuir film balance approach. This approach is particularly well suited for investigation of in-plane interactions among different lipid species and has been used extensively to investigate the interaction of cholesterol with different sphingo- and phospholipids.[29-36] The results show that the dipole moment of *N*-14:0 DMPE is higher than that of DMPE and that mixing *N*-14:0 DMPE with either cholesterol or Ca^{2+} significantly affects the resulting in-plane packing elasticity.

Materials and Methods

Materials

DMPE was obtained from Avanti Polar Lipids (Alabaster, AL). Myristic acid was a product of Sigma (St. Louis, MO). Oxalyl chloride was obtained from Lancaster Synthesis Ltd. (Eastgate, U.K.). Cholesterol was purchased from NuChek (Elysian, MN).

Synthesis of *N*-14:0 DMPE

Myristoyl chloride was synthesized by the reaction of 4 mol equiv of oxalyl chloride with 1 mol equiv of myristic acid as described.[26] *N*-Myristoyl DMPE was synthesized by the reaction of DMPE with myristoyl chloride, converted to the sodium salt, and partially purified by acetone precipitation, essentially as described earlier.21,[26] The product was further purified by column chromatography on a Lichroprep Si60 column (40-65 mesh size) (E. Merck, Germany) using successively dichloromethane/methanol/water (200/15/1, v/v) and dichloromethane/methanol/water (100/15/1, v/v) as the eluting solvents. Elution was monitored by thin-layer chromatography (TLC), and fractions corresponding to pure *N*-14:0 DMPE were pooled and concentrated by rotary evaporation. Traces of water were removed by passing the solution through anhydrous Na_2SO_4. The solvent was then removed by further rotary evaporation, and the last traces of solvent were removed by vacuum desiccation. Purity of the product was checked by TLC on silica gel using dichloromethane/methanol/aqueous NH_3 (65/25/4, v/v) as the solvent. Final stock concentrations of *N*-14:0 DMPE and DMPE were determined by phosphate analysis,[37] whereas cholesterol stocks were determined gravimetrically (Cahn 4700 microbalance).

Monolayer Conditions

Stock lipid solutions were prepared by dissolving lipids in hexane/isopropanol/water (70/30/2.5). Solvent purity was verified by dipole potential measurements.[38] Water for the subphase buffer was purified by reverse osmosis, activated charcoal adsorption, and mixed-bed deionization and then passed through a Milli-Q UV Plus System (Millipore Corp., Bedford, MA) and filtered through a 0.22 μm Millipak 40 Membrane. Subphase buffer (pH 6.6) consisting of 10 mM HEPES(Na), 100 mM NaCl, and 0.2% NaN_3 was stored under argon until use.

Surface pressure-molecular area-surface potential (π-*A*) isotherms were measured using a computer-controlled Langmuir type film balance, calibrated according to the equilibrium spreading pressures of known lipid standards.[39] Lipids were dissolved (51.67 μL aliquots) and spread in hexane/isopropanol/water (70:30:2.5). Films were compressed at a rate of ≤4 $Å^2$/molecule/min after an initial delay period of 4 min. The subphase was maintained at a fixed temperature using a thermostated circulating water bath. Dipole potentials were measured using a ^{210}Po ionizing electrode. The film balance was housed in an isolated laboratory supplied with clean air by a Bioclean Air Filtration system equipped with charcoal and HEPA filters. The trough was separately enclosed under humidified argon, cleaned with a seven-stage series filtration setup consisting of an Alltech activated charcoal gas purifier, a LabClean filter, and a series of Balston disposable filters consisting of two adsorption (carbon) and three filter units (93% and 99.99% efficiency at 0.1 μm). Other features that contribute to isotherm reproducibility include automated lipid spreading via a modified HPLC autoinjector, automated surface cleaning by multiple barrier sweeps between runs, and highly accurate and reproducible setting of the subphase level by an automated aspirator.[40,41]

Analysis of Isotherms

In keeping with recent proposals, we avoid using the term “liquid condensed” and instead use the term “condensed” to denote monolayer states in which the hydrocarbon chains are ordered.[42] The “liquid-expanded” state differs from the condensed state in that the chains are conformationally disordered. Monolayer phase transitions between the liquid-expanded and condensed states were identified from the second and third derivatives of surface pressure (π) with respect to molecular area (*A*).[43]

The dipole potential versus cross-sectional molecular area (Δ*V*-*A*) behavior can be described by

$$\Delta V = 37.7\mu_{\perp}/A + \Delta V_0$$

where ΔV is the potential measured in millivolts, and $\mu\perp$ is the dipole moment (in millidebyes) perpendicular to the lipid-water interface and can be determined from the slope of ΔV versus $1/A$ plots (see, e.g., refs 44 and 45). The intercept term, ΔV_0, has been shown to be lipid-specific and appears to arise from an epitaxial ordering of interfacial water molecules.[44,46] ΔV versus $1/A$ plots of various liquid-expanded lipids are linear up to surface pressures where the second derivative of the π-A isotherms ($d^2\pi/dA^2$) goes from positive to negative values (π_d).[44] The linearity indicates a lack of significant dipole reorientation over the range of surface pressures leading up to π_d and typically encompasses 80-90% of the π-A data for liquid-expanded films.

Monolayer compressibilities at the indicated experimental mixing ratios were obtained from π-A data using

$$C_s = (-1/A)\,(dA/d\pi) \tag{1}$$

where A is the area per molecule at the indicated surface pressure and π is the corresponding surface pressure (cf. refs 47 and 48). Data were expressed as the inverse function (C_s^{-1}), defined as the surface compressional modulus by Davies and Rideal,47 to facilitate comparisons with elastic moduli of area compressibility data in bilayer systems (e.g., see refs 49 and 50). We used a 100 point sliding window that utilized every fourth point to calculate a C_s^{-1} value prior to advancing the window 1 point. Decreasing the window to 25 points gave similar results. Each C_s^{-1} versus average molecular area curve consisted of 200 C_s^{-1} values obtained at equally spaced molecular areas along the π-A isotherms. The standard error of the C_s^{-1} values is about 2%. High C_s^{-1} values correspond to low in-plane elasticity among packed lipids in a monolayer.

Analysis of *N*-14:0 DMPE and Cholesterol Mixtures

The area condensing effect of cholesterol on *N*-14:0 DMPE was determined from plots of average molecular area versus composition.[36] Experimentally observed areas of the mixtures were compared with areas calculated by summing the molecular areas of the pure components (apportioned by mole fraction in the mixture). The calculated average molecular area (A) of two-component mixtures was determined at a given surface pressure (π) by using the following equation:

$$A = X_1\,(A_1) + (1 - X_1)\,(A_2) \tag{2}$$

where X_1 is the mole fraction of component 1 and A_1 and A_2 are the molecular areas of pure components 1 and 2 at identical surface pressures. Negative deviations from additivity indicate area condensation and imply intermolecular accommodation and/or dehydration interactions between the lipids in the mixed films.[51]

To complement the area condensation data, monolayer compressibilities (C_s) were obtained from π-A data at the indicated experimental mixing ratios by using eq 1 (described above). Ideal mixing was modeled by apportioning the C_s value for each lipid (as a pure entity) by both molecular area fraction and mole fraction as described previously.33,36 Thus, at a given constant surface pressure (π),

$$C_s = (1/A)\,[(C_{s1}A_1)\,X_1 + (C_{s2}A_2)\,X_2] \tag{3}$$

where X_2) (1 - X_1) and C_s is additive with respect to the product $C_{si}A_i$ rather than C_{si} for either ideal or completely nonideal mixing. Deviations of experimental values from calculated ideality indicate that the lipid components of the mixed monolayers are partially nonideally mixed. Data were again expressed in terms of the surface compressional modulus (C_s^{-1}),47 to facilitate comparisons with elastic moduli of area compressibility determinations in bilayer systems (cf. refs 49 and 50). As shown by Smaby et al.,36 the C_s^{-1} values of PC-cholesterol mixed monolayers are strongly affected by PC acyl structure. When mixed with equivalent high cholesterol mole fractions, PCs with saturated acyl chains have much higher C_s^{-1} values (lower in-plane elasticity) than PCs with unsaturated acyl chains suggesting that cis double bonds can act as interfacial "springs" that control the cholesterol-induced reduction in in-plane elasticity. We found pure cholesterol monolayers, which are highly condensed, to have C_s^{-1} values of 1126, 1551, and 1540 mN/m at 10, 20, and 30 mN/m, respectively, in agreement with Merkel and Sackmann.[52] For additional discussion of membrane micro-mechanical properties and of elasticity in two dimensions, readers are referred to Needham[53] and Behroozi,[48] respectively.

Results

Pure *N*-14:0 DMPE Behavior

To determine whether the *N*-myristoyl chain that is covalently linked to the PE headgroup aligns with the two *O*-myristoyl chains at the air-water interface, the surface pressure versus average molecular area (π-*A*) behavior was measured using a Langmuir type film balance. Figure 1A shows force-area isotherms obtained at 24 °C for *N*-14:0 DMPE and for DMPE on a subphase containing 100 mM NaCl. Notably, "lift-off" and collapse of *N*-14:0 DMPE occur near 126 Å^2 per molecule and between 59 and 61 Å^2 per molecule, respectively, whereas lift-off and collapse of DMPE occur near 80 Å^2 per molecule and between 38 and 39 Å^2 per molecule, respectively. Because the cross-sectional areas of saturated hydrocarbon chains are known to be ~19-20 Å2 per chain,[54] we suggest that the *N*-14:0 chain of *N*-14:0 DMPE does not localize to the aqueous subphase but rather aligns roughly parallel with the two ester-linked acyl chains at the air-water interface.

At 24 °C, the π-*A* isotherm of *N*-14:0 DMPE shows a liquid-expanded to condensed (LE-C) phase transition with an onset surface pressure near 10 mN/m, which is similar to that of DMPE (Figure 1A). A higher order transition also occurs near 28 mN/m for *N*-14:0 DMPE and near 32 mN/m for DMPE (Figure 1A, arrows). Measurements performed at different fixed temperatures in the 15-30 °C range show that the molecular area at the onset of the LE-C phase transition varies inversely with temperature (Figure 2A). Plots of the C_s^{-1} versus average area (Figure 2B) show characteristic sharp declines in C_s^{-1} upon entering the LE-C phase coexistence region due to differences in the partial molar areas of the liquid-expanded (chain-disordered) and condensed (chain-ordered) phases (e.g., see refs 43 and 55). Small inflections in the C_s^{-1} versus average area are observed for the higher order transition of *N*-14:0 DMPE (Figure 2B).

At the onset of LE behavior (~126 Å^2 per molecule), the surface potential (Δ*V*) of *N*-14:0 DMPE is ~200 mV and rises steadily with film compression. Upon reaching the cross-sectional area corresponding to onset of the LE-C phase transition (~96 Å^2 per molecule), Δ*V* is about 250 mV. With further compression, the Δ*V*-*A* slope continues to increase until collapse begins near 380 mV. In contrast, with DMPE Δ*V* is about 300 mV at the onset of LE behavior (~80 Å^2 per molecule) and continuing compression results in a steadily increasing Δ*V*. At 60Å^2 per molecule when the LE-C phase transition begins, Δ*V* is about 370 mV. With further compression, the Δ*V*-*A* slope changes suddenly, with Δ*V* rising more steeply until collapse begins at ~540 mV. Analyses of the surface potential versus inverse molecular area reveal nonzero *y*-intercepts (ΔV_0) as well as differences in the dipole moments ($\mu_\perp$) perpendicular to

the air-water interface (Table 1). Notably, $\mu_{\perp}$ values for *N*-14:0 DMPE are higher than those of DMPE.

Because *N*-acylation of DMPE's headgroup shifts the net charge from zwitterionic to negative at physiological pH, the effect of calcium ions on force-area behavior was investigated. Figure 1 shows that including Ca^{2+} (2 mM) in the subphase beneath *N*-14:0 DMPE lowered its lift-off area from ~126 to ~116 $Å^2$ per molecule, increased its lift-off ΔV by ~20 mV, lowered its collapse area by ~2$Å^2$ per molecule, and raised its collapse ΔV by ~35 mV. Also, a 4-5 mN/m decrease in the LE-C transition onset pressure was observed along with a 25 mV increase in ΔV. The preceding shifts occurred even though 100 mM NaCl was present in the subphase along with the 2 mM $CaCl_2$. In this regard, it is noteworthy that including EGTA in the subphase in the absence of Ca^{2+} had no effect on isotherm behavior indicating that the lipid preparation is free of any divalent cations (data not shown).

N-14:0 DMPE and Cholesterol Mixtures

To assess interactions between cholesterol and *N*-14:0 DMPE, π-*A* behavior was measured in mixtures containing increasing mole fractions of cholesterol and compared with that of DMPE-cholesterol mixtures (Figure 3). Changes induced by cholesterol were analyzed by calculating area condensations, that is, average molecular area versus composition, and by determining the impact on in-plane elasticity, that is, C_s^{-1} versus average molecular area and C_s^{-1} versus composition.

Figure 3A shows that cholesterol slightly elevates the onset pressure of the *N*-14:0 DMPE LE-C phase transition, which is visible at low cholesterol mole fractions ($\leq$0.3) but then disappears at higher sterol mole fractions. Similar behavior is observed for DMPE except that less cholesterol is required to eliminate the LE-C phase transition (Figure 3B). This is more clearly seen in the C_s^{-1} versus average molecular area plots where the “trough” or dip characteristic of LE-C phase coexistence provides a more sensitive measure of the LE-C transition. The data in Figure 3 also show that the average cross-sectional area in the *N*-14:0 DMPE-cholesterol mixed monolayers decreases as the cholesterol content increases. This behavior is not surprising given that pure cholesterol behaves as a relatively small component with a relatively fixed area (36-38 $Å^2$ per molecule) compared to pure *N*-14:0 DMPE.

To determine whether cholesterol exerts an ordering effect on the acyl chains of *N*-14:0 DMPE, we analyzed the mean molecular area versus cholesterol content. Parts A and B of Figure 4 show the results at three different surface pressures (5, 20, and 35 mN/m) for *N*-14:0 DMPE and DMPE, respectively. Solid lines represent ideal additivity calculated from the cross-sectional molecular areas of pure cholesterol and *N*-14:0 DMPE (or DMPE) and apportioned by mole fraction. In Figure 4A,B, large negative deviations from additivity are evident at 5 mN/m, a surface pressure producing chain-disordered, liquid-expanded behavior in the absence of cholesterol. Notably, for *N*-14:0 DMPE the cholesterol-induced negative deviations from additivity, that is, area condensations, steadily increase with increasing cholesterol until reaching maximum deviation (19.1%) near equimolar sterol, whereas for DMPE, maximum deviation is achieved by 0.35 cholesterol (23.8%) and then diminishes as sterol mole fraction continues to increase. No negative deviations from additivity are observed at 20 or 35 mN/m, surface pressures that result in chain-ordered, condensed behavior in the absence of cholesterol. Rather, slight positive deviations from additivity occur at 20 and 35 mN/m, especially for *N*-14:0 DMPE. Thus, cholesterol exerts a significant ordering effect on *N*-14:0 DMPE's and DMPE's liquid-expanded phases but not on their condensed phases.

To gain additional insights into mixing behavior at high surface pressures (>30 mN/m) that mimic the lipid cross-sectional areas of biomembranes, the surface compressional moduli were analyzed as a function of cholesterol mole fraction. In contrast to monolayer area

condensations, which provide maximal response at lower surface pressures, surface compressional moduli respond maximally at higher surface pressures.[35,56] Parts A and B of Figure 5 show c_s^{-1} versus composition plots for *N*-14:0 DMPE and DMPE, respectively. Because of our interest in cholesterol mole fractions most common in biological membranes, we have focused on the 0-0.6 sterol mole fraction range. Solid lines represent theoretical ideal mixing calculated from the c_s^{-1} values of pure cholesterol and *N*-14:0 DMPE (or DMPE) and apportioned by both mole and area fraction.[33,36] Because of this apportioning, the theoretical ideal mixing lines are nonlinear. The higher the c_s^{-1} value, the lower the interfacial elasticity. In the absence of cholesterol, the c_s^{-1} values reflect the in-plane elastic interactions characteristic of the *N*-14:0 DMPE and DMPE phase states. As a result, the c_s^{-1} values are low at 5 mN/m when the lipids are chain-disordered (liquid-expanded) but are elevated considerably at 35 mN/m when the lipids are chain-ordered (condensed). Notably, the c_s^{-1} value associated with the *N*-14:0 DMPE is about 1.5-fold higher than that of DMPE at 35 mN/m, a surface pressure that is thought to mimic the biomembrane situation.[57,58]

Increasing cholesterol has decidedly different effects on *N*-14:0 DMPE and DMPE. At low surface pressures (e.g., 5 mN/m), the in-plane elasticities are relatively unaffected and closely follow theoretical ideal mixing (Figure 5A,B, lower solid lines) until sterol mole fractions exceed 0.3 in *N*-14:0 DMPE and 0.2 in DMPE. Thereafter, increasing cholesterol produces c_s^{-1} values that show significant positive deviation from theoretical ideal mixing with experimental values of equimolar DMPE-cholesterol being 3-fold higher than those of equimolar *N*-14:0 DMPE-cholesterol. At high surface pressure (e.g., 35 mN/m), the already high c_s^{-1} values of chain-ordered, condensed phase *N*-14:0 DMPE follow theoretical ideal mixing (Figure 5A, upper solid line) and increase modestly (~60 mN/m) until cholesterol mole fractions exceed 0.1. Then, C_s^{-1} values decrease until achieving a minimum near 0.4 mole fraction cholesterol. The minimum is ~275 mN/m negative with respect to theoretical ideal mixing. Between 0.4 and 0.6 mole fraction sterol, C_s^{-1} values rise but still remain negative relative to theoretical ideal mixing behavior.

In contrast, the C_s^{-1} values of DMPE-cholesterol mixtures show only slight deviations from theoretical ideal mixing behavior at 35 mN/m (Figure 5B, upper solid line). Between cholesterol mole fractions of 0.1 and 0.4, slight negative deviations are evident compared to the slight positive deviations that occur between cholesterol mole fractions of 0.4 and 0.6.

Discussion

Monolayer Properties of *N*-14:0 DMPE

Previous studies employing ^{31}P NMR, FTIR, and spin-label ESR have indicated that the *N*-acyl chains of NAPEs fold back and incorporate into the hydrophobic interior of the membrane, when the length of the *N*-acyl chains is around 10 C atoms or longer.[21,24,27] The π-*A* isotherms in Figure 1 show that the area per molecule of DMPE increases by a factor of 1.5 both at monolayer lift-off and at collapse when the phosphorylethanolamine group is acylated with a long myristoyl chain. These results indicate that the *N*-acyl chain of *N*-14:0 DMPE is embedded in the hydrophobic interior of the lipid monolayer and are consistent with previous spin-label ESR studies,[27] which have shown that the *N*-acyl chain is oriented parallel to the *O*-acyl chains in bilayer membranes. Because the molecular areas of saturated acyl chains are 19-20 Å^2 per molecule,[54] the 59-61 Å^2 per molecule value at monolayer collapse pressure is consistent with the *N*-acyl chain of *N*-14:0 DMPE being aligned with the two ester-linked (*O*-) acyl chains.

The onset pressure for the liquid-expanded to condensed phase transition of *N*-14:0 DMPE is nearly identical to that observed for DMPE (Figure 1). Addition of a third saturated acyl chain would normally be expected to decrease the onset pressure for the LE-C phase transition by enhancing attractive interactions among molecules due to the increase in hydrocarbon chains

per polar headgroup. Yet, *N*-acylation of the phosphorylethanolamine headgroup renders *N*-14:0 DMPE's headgroup net negatively charged, which is expected to promote repulsive interactions among neighboring lipids. Thus, in the presence of 100 mM NaCl, the changes due to acylation appear to compensate those due to intermolecular hydrogen bonding along with any contributions from the change in net charge. Notably, the chain-melting transition temperatures of aqueous dispersions of diacyl PEs show similar behavior upon *N*-acylation.[26] For diacyl PEs with identical saturated *O*-acyl chains, addition of an *N*-acyl chain of matched chain length increases the chain-melting enthalpy as compared to the parent diacyl PEs. However, the transition temperature remains constant due to enthalpy-entropy compensation.[26]

The surface potential data reveal a significant increase (~80 mD) in *N*-14:0 DMPE's net dipole moment ($\mu_\perp$) compared to that of DMPE in both the chain-disordered (liquid-expanded) and chain-ordered (condensed) phase states (Table 1). Because the subphase used in our monolayer studies contained 100 mM NaCl, the electro-static contribution arising from the negatively charged phosphate group of *N*-14:0 DMPE is expected to be reduced by 90% in our surface potential data.[59] Yet, Brockman[46] previously showed that it is the ΔV_0 contribution, not $\mu_\perp$, of monolayer surface potential, that is affected by changing salt concentration in the subphase. The higher *N*-14:0 DMPE $\mu_\perp$ compared to that of DMPE suggests different average orientations of the permanent dipoles in the interfacial region. This finding is consistent with previous IR studies in which the carbonyl and amide bands of *N*-16:0 DPPE and DPPE were carefully evaluated with respect to intermolecular hydrogen bonding.[25] While the amine of DPPE is located near the bilayer surface, the amide group of *N*-16:0 DPPE appears to be located closer to the interfacial region possibly due to the anchoring effect of the *N*-acyl chain in the hydrophobic region. Locating the amide linkage in a low dielectric region could substantially increase its dipole potential. With the amide oxygen pointing toward the aqueous phase, the resulting dipole potential would be more positive inside the hydrocarbon region, analogous to the ester group situation of *O*-linked acyl chains in diacyl PC (see, e.g., refs 46 and 60).

Effect of Ca^{2+} Ions

Because *N*-acylation shifts DMPE's net charge from zwitterionic to negative and because Ca^{2+} is known to bind to negatively charged lipids and change their phase behavior,[61] it is not surprising that Ca^{2+} has a condensing effect on *N*-14:0 DMPE monolayer behavior (Figure 1A). What is notable is that the Ca^{2+}-induced changes are evident in the presence of 100 mM NaCl and differ in important ways from those achieved by lowering temperature (Figure 2). For instance, 2 mM Ca^{2+} had a much greater impact on the surface compressional moduli (C_s^{-1}) at biomembrane-like surface pressures. The C_s^{-1} of *N*-14:0 DMPE increased from 560 to 726 mN/m at 30 mN/m when 2 mM Ca^{2+} was included in the 24 °C subphase, whereas the C_s^{-1} increased from 560 to 620 mN/m as a result of shifting subphase temperature from 24 to 20 °C. In addition, *N*-14:0 DMPE's two-dimensional (2D) transition was affected differently by Ca^{2+} compared to lowering temperature. The onset surface pressure of *N*-14:0 DMPE's 2D transition decreased by 4-5 mN/m in the presence of 2 mM Ca^{2+} while leading to only a slight increase (~1.5 $Å^2$ per molecule) in the 2D-transition onset average molecular area. In contrast, reducing temperature from 24 to 20 °C (in the absence of Ca^{2+}) decreased *N*-14:0 DMPE's 2D-transition onset surface pressure by ~7.5 mN/m while increasing the 2D-transition onset average molecular area by ~10-11 $Å^2$ per molecule (Figure 2). Taken together, these observations suggest that Ca^{2+} ions primarily affect the headgroup region of NAPE. In bilayer systems, the interaction of Ca^{2+} ions with NAPEs also significantly impacts phase behavior. Freeze-fracture EM studies have shown that *N*-16:0 DOPE exists in the hexagonal phase at 55 °C in the presence of Ca^{2+}, whereas the lipid is in the bilayer phase at the same temperature in the absence of Ca^{2+}.[20] Shangguan et al.[62] showed that placing *N*-12:0 DOPE in DOPC provides a Ca^{2+}-dependent trigger for fusing the stable liposomes with either erythrocyte ghosts or

nucleated U-937 cells. Our monolayer results provide further evidence that hexagonal phase induction by NAPEs is most likely due to modifications that occur at the headgroup rather than at the acyl chain region.

Mixtures of *N*-14:0 DMPE and Cholesterol

The effect of cholesterol on the acyl chain packing of phosphoand sphingolipids has been widely studied, and it is well established that cholesterol induces condensation of the acyl chains of phospholipids such as PC and PE. The negative deviations from additivity seen in the plots of mean molecular areas versus mole fraction of cholesterol (Figure 4) at a surface pressure of 5 mN/m for both *N*-14:0 DMPE and DMPE indicate that cholesterol has a significant ordering effect on the chain-disordered, liquid-expanded state of both lipids. Since the positive deviations seen at 20 and 35 mN/m are rather small (Figure 4), it appears that cholesterol has no ordering effect on the condensed phases of these two lipids.

Because *N*-14:0 DMPE has three acyl chains and DMPE has two acyl chains, we analyzed the per chain interaction with cholesterol. Figure 6 shows the result of subtracting the data in Figure 4B (DMPE-cholesterol) from the data in Figure 4A (*N*-14:0 DMPE-cholesterol). The resulting data for 5 mN/m are especially interesting because they suggest that the presence of a third acyl chain does not enhance the sterol-induced condensation process any more than what is achieved with two acyl chains. Stated another way, at low cholesterol mole fractions, on average, full interaction of cholesterol with *N*-14:0 DMPE requires only two of the three acyl chains. This could be the result of *N*-acyl PE having a triagonal molecular shape with respect to the arrangement of its three acyl chains versus the planar shape of cholesterol's ring. Since monolayer data report average molecular behavior, it is not possible to identify which of the acyl chains interact specifically with cholesterol. Furthermore, ESR studies involving 40 mol % cholesterol indicate that the spin-labeled *N*-acyl chain of NAPE and the spin-labeled *sn*-2 chain of DMPC experience similar ordering effects by cholesterol in DMPC/cholesterol and *N*-14:0 DMPE/cholesterol host matrixes.[27]

The surface compressional moduli (C_s^{-1}) for the mixtures of cholesterol with *N*-14:0 DMPE and DMPE at different surface pressures, given in Figure 5, show similar general trends in the surface pressure range of 5-20 mN/m. The abrupt positive deviations from theoretical ideal mixing behavior represent a pattern that has been observed previously in saturated PCs[36] and appears to be consistent with the onset of liquid-ordered phase structure that may contain condensed lipid complexes.[59,63] At 35 mN/m, the C_s^{-1} values are relatively high for *N*-14:0 DMPE and, above 0.1 mole fraction, cholesterol lowers those C_s^{-1} values especially with respect to the behavior predicted by theoretical ideal mixing. In contrast, for DMPE the C_s^{-1} values increase only slightly up to 30 mol % cholesterol values increase only slightly up to 30 mol % cholesterol and then gradually and steadily rise between 30 and 60 mol % cholesterol, deviating only marginally from theoretical ideal mixing. Overall, the behavior observed with *N*-14:0 DMPE-cholesterol mixtures suggests that cholesterol mole fractions above 0.1 provide no additional “ordering” effect on the already highly ordered *N*-14:0 DMPE. The substantial drop in the C_s^{-1} values between 0.1 and 0.4 mole fraction sterol indicates a significant disordering effect that might represent a coexistence region of relatively immiscible solid phases. Such a possibility appears feasible given cholesterol's marked equilibrium partitioning preference for a two-chain lipid such as egg PC compared to a three-chain lipid such as triolein.[64] Of course, additional studies of *N*-14:0 DMPE and cholesterol mixtures will be required to fully evaluate the preceding ideas.

Biotechnological and Physiological Implications

The ability of NAPEs to stabilize liposomes suggests that they would be very useful in developing liposomal drug delivery agents.[18,19] The present results show that *N*-14:0 DMPE

exhibits a high lateral area compressibility modulus and suggest that the presence of NAPE might result in a rigidification of the lipid membrane and reduce permeability and decrease leakage of contents, as observed by Domingo et al.[18] and Mercadal et al.[19]

The content of NAPEs in different biological tissues increases in response to stress.[1,14-16] This can lead to the increase in the content of NAEs, produced by the degradation of the former class of lipids by a phospholipase D type enzyme. The resulting NAEs can serve as neuro-transmitters/second messengers. NAPEs also modulate the activity of membrane-bound enzymes such as β-glucocerebrosidase.[65] The phospholipase D that acts on NAPEs to produce NAEs is a membrane-associated protein and requires the presence of the *N*-acyl chain for catalytic activity and does not degrade PC or PE.[66] Thus, it appears plausible that the modulation of certain membrane-bound enzymes by NAPEs may be related to the alteration of in-plane elasticity moduli, resulting from *N*-acylation of PE.

Acknowledgments

Work done at the University of Hyderabad was supported by a research grant from the Department of Science and Technology, Government of India (to M.J.S.). M.R. is a Senior Research Fellow of the CSIR, Government of India. Investigations carried out at the Hormel Institute were supported by the Hormel Foundation and by USPHS Grants HL49180 (to H.L.B.) and GM45928 (to R.E.B.).

Abbreviations

PC	phosphatidylcholine
PE	phosphatidylethanolamine
DLPE, DMPE, DPPE	1,2-dilauroyl-, 1,2-dimyrstoyl-, 1,2-dipalmitoyl-*sn*-glycero-3-phosphoethanolamine
NAE	*N*-acylethanolamine
NAPE or *N*-acyl PE	*N*-acylphosphatidylethanolamine
***N*-12:0 DLPE**	1,2-dilauroyl-*sn*-glycero-3-(*N*-lauroyl)-phosphoethanolamine
***N*-14:0 DMPE or *N*-myristoyl DMPE**	1,2-dimyristoyl-*sn*-glycero-3-(*N*-myristoyl)-phosphoethanolamine
***N*-16:0 DPPE or *N*-palmitoyl DPPE**	1,2-dipalmitoyl-*sn*-glycero-3-(*N*-palmitoyl)-phosphoethanolamine
***N*-6:0 DPPE**	1,2-dipalmitoyl-*sn*-glycero-3-(*N*-hexyl)-phosphoethanolamine
EM	electron microscopy
DSC	differential scanning calorimetry
NMR	nuclear magnetic resonance
ESR	electron spin resonance
FTIR	Fourier transform infrared reflectance
ATR	attenuated total reflectance

References

(1). Schmid HHO, Schmid PC, Natarajan V. Prog. Lipid Res 1990;29:1. [PubMed: 2087478]
(2). Bomstein RA. Biochem. Biophys. Res. Commun 1965;21:49. [PubMed: 5865490]

(3). Aneja R, Chadha JS, Knaggs JA. Biochem. Biophys. Res. Commun 1969;36:401. [PubMed: 5387722]
(4). Dawson RMC, Clarke N, Quarles RH. Biochem. J 1969;114:265. [PubMed: 5810083]
(5). Matsumoto M, Miwa M. Biochim. Biophys. Acta 1973;296:350. [PubMed: 4688439]
(6). Gray GM. Biochim. Biophys. Acta 1976;431:1. [PubMed: 1268235]
(7). Clarke NG, Hazlewood GP, Dawson RMC. Chem. Phys. Lipids 1976;17:222. [PubMed: 991380]
(8). Somerharzu P, Renkonen O. Biochim. Biophys. Acta 1979;573:83. [PubMed: 454642]
(9). Hargin KD, Morrison WR. J. Sci. Food Agric 1980;31:877.
(10). Epps DE, Natarajan V, Schmid PC, Schmid HHO. Biochim. Biophys. Acta 1980;618:420. [PubMed: 7397206]
(11). Natarajan V, Schmid PC, Reddy PV, Zuzarte-Augustin ML, Schmid HHO. Biochim. Biophys. Acta 1985;835:426. [PubMed: 4016139]
(12). Natarajan V, Schmid PC, Schmid HHO. Biochim. Biophys. Acta 1986;878:32. [PubMed: 3730413]
(13). Schmid HHO, Schmid PC, Natarajan V. Chem. Phys. Lipids 1996;80:133. [PubMed: 8681424]
(14). Berdyshev EV, Schmid PC, Dong Z, Schmid HHO. Biochem. J 2000;346:369. [PubMed: 10677355]
(15). Hansen HS, Lauritzen L, Moesgaard B, Strand AM, Hansen HH. Biochem. Pharmacol 1998;55:719. [PubMed: 9586943]
(16). Hansen HS, Moesgaard B, Hansen HH, Schousboe A, Petersen G. Lipids 1999;34:S327. [PubMed: 10419193]
(17). Chapman KD, Tripathy S, Venables B, Desouza AD. Plant Physiol 1998;116:1163. [PubMed: 9501149]
(18). Domingo JC, Mora M, de Madariaga MA. Biochim. Biophys. Acta 1993;1148:308. [PubMed: 8504125]
(19). Mercadal M, Domingo JC, Bermudez M, Mora M, De Madariaga MA. Biochim. Biophys. Acta 1995;1235:281. [PubMed: 7756336]
(20). Newman JL, Stiers DL, Anderson WH, Schmid HHO. Chem. Phys. Lipids 1986;42:249. [PubMed: 3829207]
(21). Akoka S, Tellier C, LeRoux C, Marion D. Chem. Phys. Lipids 1988;46:43.
(22). Domingo JC, Mora M, de Madariaga MA. Chem. Phys. Lipids 1995;75:15.
(23). Marsh D, Swamy MJ. Chem. Phys. Lipids 2000;105:43. [PubMed: 10727113]
(24). Lafrance D, Marion D, Peézolet M. Biochemistry 1990;29:4592. [PubMed: 2372544]
(25). Lafrance C-P, Blochet J-E, Pezolet M. Biophys. J 1997;72:2559. [PubMed: 9168031]
(26). Swamy MJ, Marsh D, Ramakrishnan M. Biophys. J 1997;73:2556. [PubMed: 9370449]
(27). Swamy MJ, Ramakrishnan M, Angerstein B, Marsh D. Biochemistry 2000;39:12476. [PubMed: 11015229]
(28). Ramakrishnan M, Marsh D, Swamy MJ. Biochim. Biophys. Acta 2001;1512:22. [PubMed: 11334621]
(29). Lund-Katz S, Laboda HM, McLean LR, Phillips MC. Biochemistry 1988;27:3416. [PubMed: 3390441]
(30). Johnston DS, Chapman D. Biochim. Biophys. Acta 1988;937:10. [PubMed: 3334840]
(31). Gronberg L, Ruan Z, Bittman R, Slotte JP. Biochemistry 1991;30:10746. [PubMed: 1931994]
(32). Slotte JP, Ostman AL, Kumar ER, Bittman R. Biochemistry 1993;32:7886. [PubMed: 8347594]
(33). Ali S, Smaby JM, Brockman HL, Brown RE. Biochemistry 1994;33:2900. [PubMed: 8130203]
(34). Smaby JM, Brockman HL, Brown RE. Biochemistry 1994;33:9135. [PubMed: 8049216]
(35). Smaby JM, Momsen MM, Kulkarni VS, Brown RE. Biochemistry 1996;35:5696. [PubMed: 8639529]
(36). Smaby JM, Momsen MM, Brockman HL, Brown RE. Biophys. J 1997;73:1492. [PubMed: 9284316]
(37). Bartlett GR. J. Biol. Chem 1959;234:466. [PubMed: 13641241]
(38). Smaby J, Brockman HL. Chem. Phys. Lipids 1991;58:249. [PubMed: 1893502]
(39). Momsen WE, Smaby JM, Brockman HL. J. Colloid Interface Sci 1990;135:547.

(40). Brockman HL, Jones CM, Schwebke CJ, Smaby JM, Jarvis DE. J. Colloid Interface Sci 1980;78:502.

(41). Brockman HL, Smaby JM, Jarvis DE. J. Phys. E: Sci. Instrum 1984;17:351.

(42). Kaganer VM, Mohwald H, Dutta P. Rev. Mod. Phys 1999;71:779.

(43). Ali S, Smaby JM, Momsen MM, Brockman HL, Brown RE. Biophys. J 1998;74:338. [PubMed: 9449334]

(44). Smaby J, Brockman HL. Biophys. J 1990;58:195. [PubMed: 2383632]

(45). Ali S, Smaby JM, Brown RE. Biochemistry 1993;32:11696. [PubMed: 8218238]

(46). Brockman H. Chem. Phys. Lipids 1994;73:57. [PubMed: 8001185]

(47). Davies, JT.; Rideal, EK. Interfacial Phenomena. 2nd ed.. Academic Press; New York: 1963.

(48). Behroozi F. Langmuir 1996;12:2289.

(49). Evans E, Needham D. J. Phys. Chem 1987;91:4219.

(50). Needham D, Nunn RS. Biophys. J 1990;58:997. [PubMed: 2249000]

(51). Cadenhead DA, Müller-Landau F. J. Colloid Interface Sci 1980;78:269.

(52). Merkel R, Sackmann E. J. Phys. Chem 1994;98:4428.

(53). Needham, D. Permeability and Stability of Lipid Bilayers. Disalvo, EA.; Simon, SA., editors. CRC Press; Boca Raton, FL: 1995. p. 49

(54). Harkins, WD. The Physical Chemistry of Surface Films. Reinhold; New York: 1952. p. 116

(55). Li X-M, Smaby JM, Momsen MM, Brockman HL, Brown RE. Biophys. J 2000;78:1921. [PubMed: 10733971]

(56). Li X-M, Momsen MM, Smaby JM, Brockman HL, Brown RE. Biochemistry 2001;40:5954. [PubMed: 11352730]

(57). MacDonald, RC. Vesicles. Rosoff, M., editor. Marcel Dekker; New York: 1996. p. 3

(58). Marsh D. Biochim. Biophys. Acta 1996;1286:183. [PubMed: 8982283]

(59). Castle JD, Hubbell WL. Biochemistry 1976;15:4818. [PubMed: 186095]

(60). Flewelling RF, Hubbell WL. Biophys. J 1986;49:541. [PubMed: 3955184]

(61). Lewis, RNAH.; McElhaney, RN. The Structure of Biological Membranes. Yeagle, P., editor. CRC Press; Boca Raton, FL: 1992. Chapter 2

(62). Shangguan T, Pak CC, Ali S, Janoff AS, Meers P. Biochim. Biophys. Acta 1998;1368:171. [PubMed: 9459596]

(63). Radhakrishnan A, Anderson RG, McConnell HM. Proc. Natl. Acad. Sci. U.S.A 2000;97:12422. [PubMed: 11050164]

(64). Sandermann H Jr. Addona GH, Miller KW. Biochim. Biophys. Acta 1997;1346:158. [PubMed: 9219898]

(65). Basu A, Prence E, Garrett K, Glew RH, Ellingson JS. Arch. Biochem. Biophys 1985;243:28. [PubMed: 3933429]

(66). Chapman KD, Lin I, DeSouja AD. Arch. Biochem. Biophys 1995;318:401. [PubMed: 7733669]

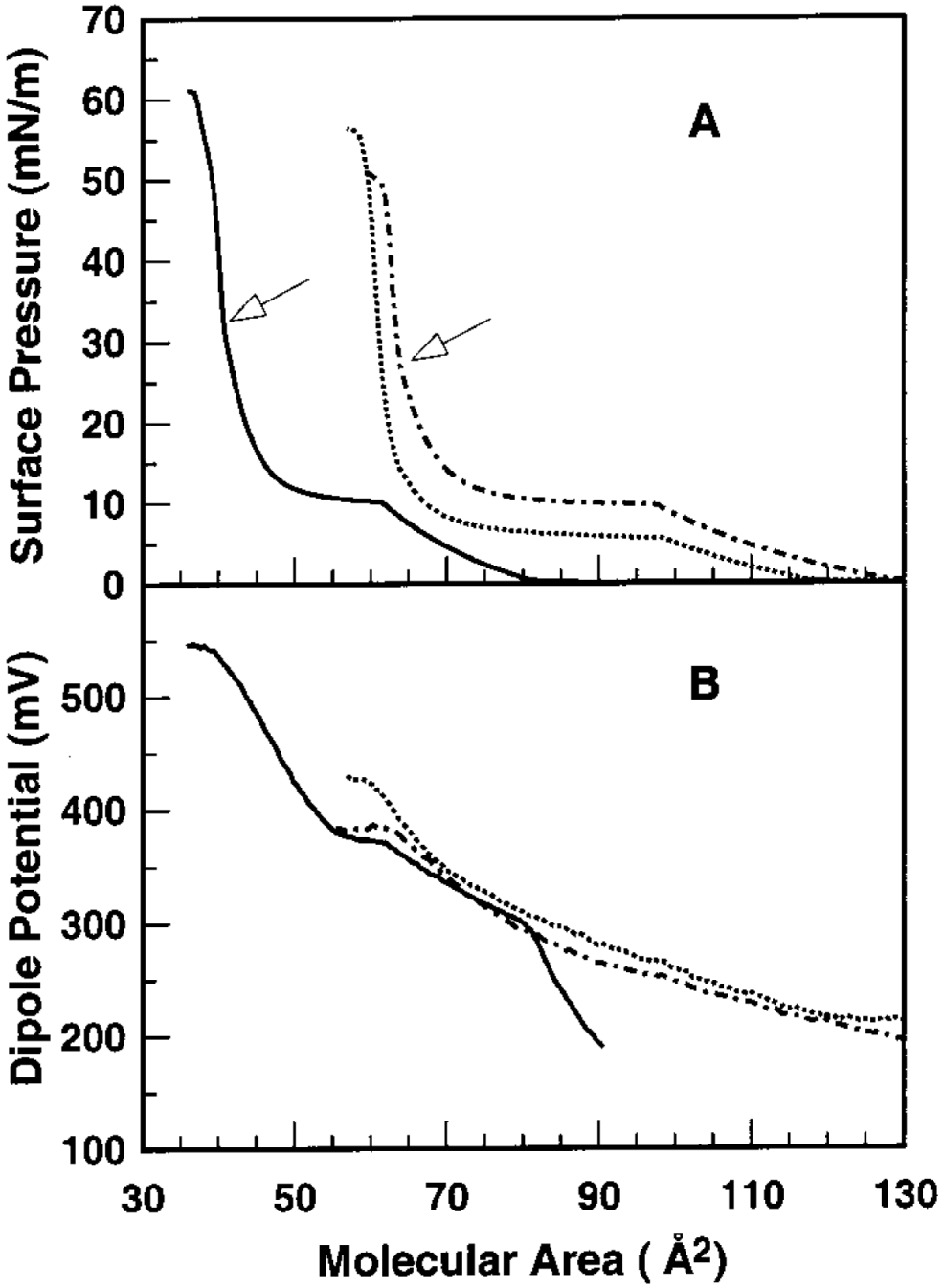

Figure 1.

(A) Surface pressure vs cross-sectional molecular area (π-*A*) and (B) dipole potential vs cross-sectional molecular area (Δ*V*-*A*) isotherms for *N*-14:0 DMPE and DMPE. Data were collected at 24 °C as described under Materials and Methods. Arrows indicate regions of higher order transitions for *N*-14:0 DMPE and DMPE. DMPE (solid line); *N*-14:0 DMPE (dashed-dotted line); *N*-14:0 DMPE + 2 mM $CaCl_2$ (dotted line).

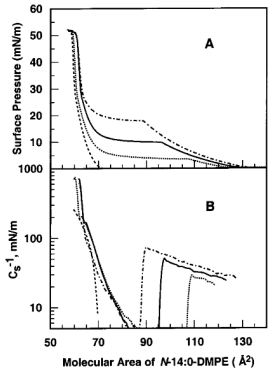

Figure 2.

Effect of temperature on *N*-14:0 DMPE interfacial behavior: (A) surface pressure vs cross-sectional molecular area (π-*A*) isotherms; (B) surface compressional modulus vs cross-sectional molecular area (C_S^{-1}-*A*) isotherms. Data were collected at 30 °C (dashed-dotted line), 24 °C (solid line), 20 °C (dotted line), and 15 °C (dashed line).

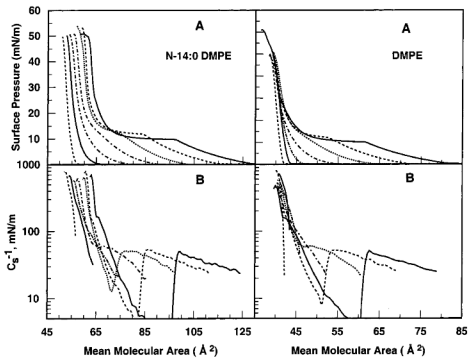

Figure 3.

Effect of cholesterol on *N*-14:0 DMPE and DMPE interfacial behavior: (A) surface pressure vs average cross-sectional molecular area (π-*A*) isotherms; (B) surface compressional modulus vs average cross-sectional molecular area (C_S^{-1}—-*A*) isotherms. Data were collected at at 24 °C. Isotherms represent cholesterol mole fractions of 0, 0.1, 0.2, 0.3, 0.4, 0.5, and 0.6 (from right to left at 5 mN/m). Matching line styles in the upper and lower panels indicate equivalent cholesterol content.

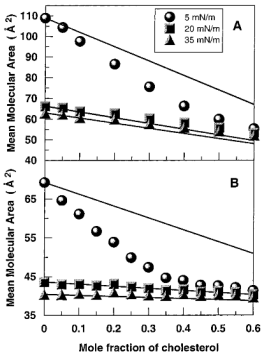

Figure 4.

Mean molecular area vs composition analyses: (A) *N*-14:0 DMPE and (B) DMPE. Data are shown at 5, 15, and 35 mN/m. Experimental data are indicated by symbols. The solid lines represent theoretical additive behavior calculated from the response of the pure lipids as described in Materials and Methods. Because the theoretical binary mixtures are apportioned by mole fraction, the response is linear.

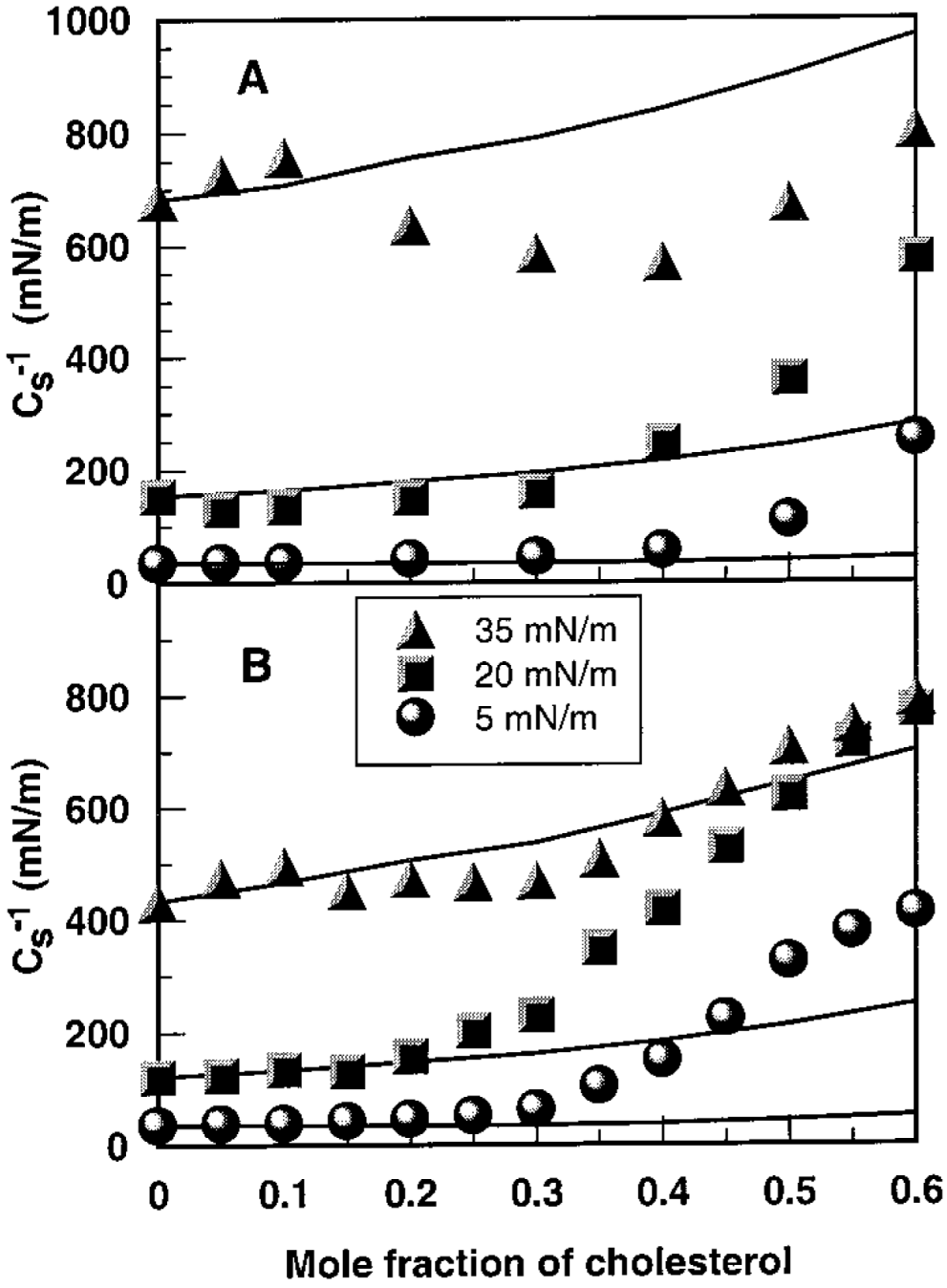

Figure 5.

Mean surface compressional modulus vs composition analyses: (A) *N*-14:0 DMPE and (B) DMPE. Data are shown at 5, 15, and 35 mN/m. Experimental data are indicated by symbols. The solid lines represent theoretical ideal behavior calculated from the response of the pure lipids as described in Materials and Methods. Because the theoretical binary mixtures are apportioned by both mole and area fractions, the response is nonlinear.

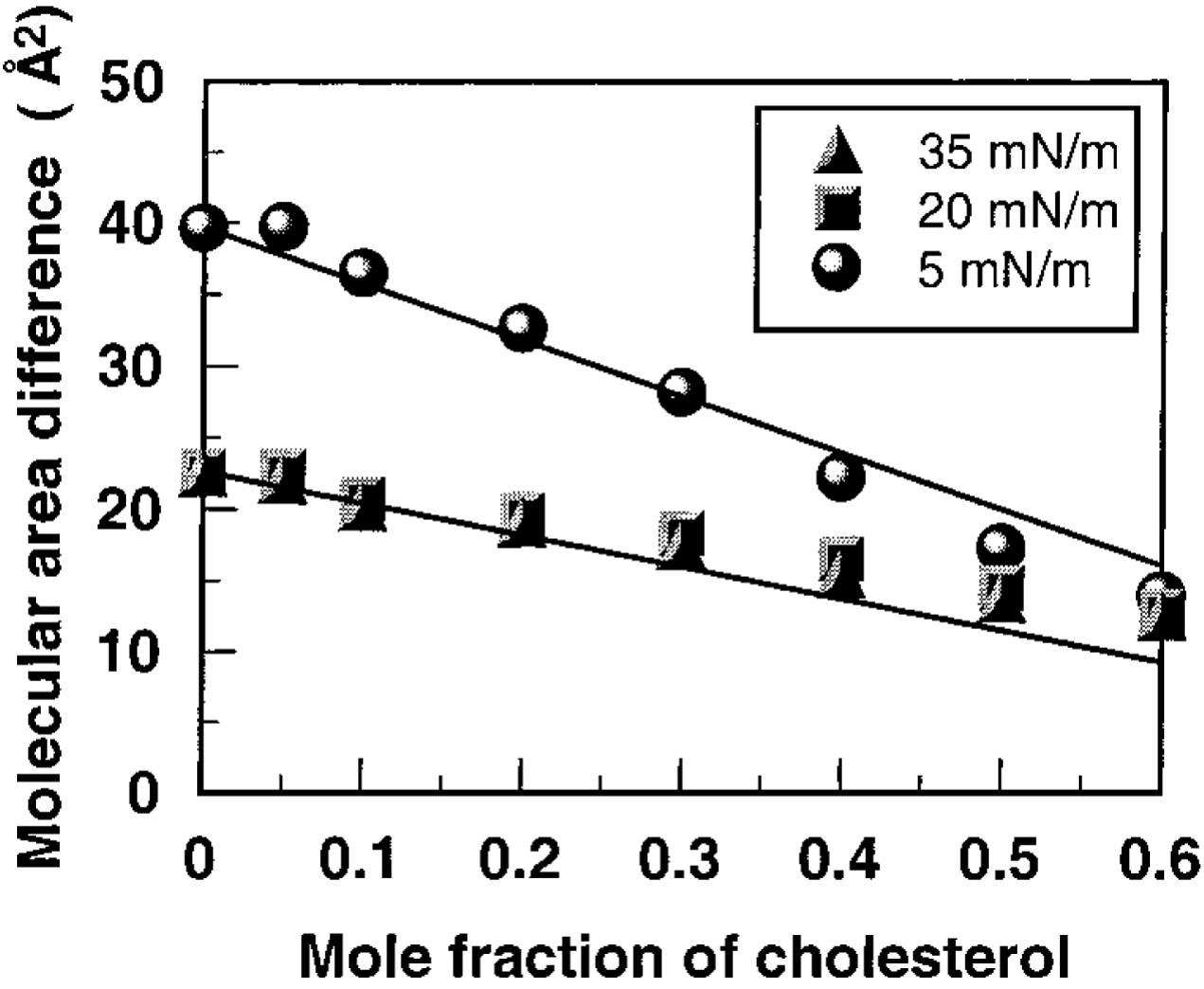

Figure 6.
Difference between the cholesterol-induced area condensation of *N*-14:0 DMPE and DMPE. Data represent a difference plot between parts A and B of Figure 4. See the Figure 4 legend for other details.

Table 1

Comparison of Parameters Related to the Dipole Potential of *N*-14:0 DMPE and DMPE[a]

	μ⊥ (mD)	ΔV_0(mV)
N-14:0 DMPE		
liquid-expanded	568	28
condensed	665	
DMPE		
liquid-expanded	490	61
condensed	619	

[a] $\mu_\perp$ = dipole moment perpendicular to the air-water interface; ΔV_0) intercept of ΔV versus I/*A* plots for the liquid-expanded and condensed phases of *N*-14:0 DMPE and DMPE (see Materials and Methods).